Silva Gabreta	vol. 24	p. 47–67	Vimperk, 2018

Modelling future hydrological pattern in a Bohemian Forest headwater catchment

Anna Lamačová[1,2,*], Jakub Hruška[1,2], Miroslav Trnka[2,4], Petr Štěpánek[2,3], Pavel Zahradníček[2,3], Jan Meitner[2] & Aleš Farda[2]

[1]Czech Geological Survey, Klárov 3, CZ-11821 Prague 1, Czech Republic
[2]Global Change Research Institute CAS, Bělidla 986/4a, CZ-60300 Brno, Czech Republic
[3]Czech Hydrometeorological Institute, Kroftova 43, CZ-61600 Brno, Czech Republic
[4]Institute of Agrosystems and Bioclimatology, Mendel University, Zemědělská 1, CZ-61300 Brno, Czech Republic
[*] anna.lamacova@geology.cz

Abstract
This study focuses on estimation of the impacts of anticipated global climate change on water balance in forested headwater catchment. The investigated catchment is located in the Šumava National Park (Bohemian Forest) in the southern part of the Czech Republic. We calculated nine future water balance scenarios for periods of 2021–2050 and 2071–2100. We used data from following models: CNRM-CM5_ALADIN53, EC-EARTH_RACMO22E, EC-EARTH_RCA4, and MPI-ESM-LR_CCLM4-8-17 with 3 emission scenarios (Representative Concentration Pathways RCP2.6, 4.5, 8.5). Corrected regional climate model daily data were used in combination with hydrological model Brook90. The scenarios projected an increase of mean annual temperature of 1.1°C (RCP4.5) and 1.4°C (RCP8.5, 2021–2050) and 2.3°C (RCP4.5) and 4.2°C (RCP8.5, 2071–2100) and increase in mean annual precipitation amount of 11% (RCP 4.5) and 15% (RCP 8.5, 2021–2050) and 15% (RCP 4.5) and 20% (RCP8.5, 2071–2100). It would result in a mean annual runoff increase of 9% (RCP4.5) and 14% (RCP8.5, 2021–2050) and 12% (RCP4.5) and 16% (RCP8.5, 2071–2100). The annual runoff cycle is projected to change significantly especially in the period of 2071–2100, when a large winter runoff increase and a spring runoff maximum decrease is expected. "Pessimistic" RCP8.5 scenarios expect even no spring runoff maxima from snowmelt and project a shift of runoff maxima to December.

Key words: climate change impact, runoff, water balance, hydrological modelling, forested catchment

Introduction

Temperature increase and changes in precipitation distribution and amounts are expected to affect hydrological pattern notably (IPCC 2007, IPCC 2013). Forested landscapes are considered to be close to the natural environment in central European conditions and the Bohemian Forest represents a large forested area of high ecological importance. Forests can be affected by climate change both directly and indirectly. Increased temperature can affect vegetation cover in forests notably even regardless of precipitation changes (Adams et al. 2009). It can lead to tree die-off or to weakening of trees and they can become more vulnerable to tree pest (Adams et al. 2009, Allen et al. 2010, Raffa et al. 2008). However, projected increases in drought frequency due to changes in precipitation and increases in stress from biotic agents (e.g. bark beetles) could further intensify tree mortality (Adams et al. 2009).

Regionally oriented studies in the Bohemian Forest documented an air temperature increase over the last century (Kliment & Matoušková 2009, Langhammer et al. 2015), however, did not detect any changes in annual or seasonal precipitation (Bernsteinová et al. 2015). Also no changes in annual runoff were found by Bernsteinová et al. (2015) and Langhammer et al. (2015), however, they noted an increase in high flows in March, which was related to significant temperature increase in late winter and early spring.

A future gradient in precipitation with an increase in the Northern Europe and decrease in the Southern Europe was projected in many studies (Forzieri et al. 2014, van Vliet et al. 2015) and runoff is expected to follow the same pattern. However, the area of central Europe lies in the transition zone, where the future precipitation changes are more ambiguous. Hanel et al. (2012) estimated changes in future hydrological pattern in area of the Czech Republic for the period of 2070–2099. According to their study runoff changes from January to May will be affected by changes in snow cover and snowmelt dynamics, with a notable shift in snowmelt from April to January–February. The summer runoff decline will be caused by summer precipitation decrease. A study from small forested headwater catchments located across the Czech Republic projected an annual runoff decrease by 15% (2021–2050) and 35% (2071–2100) (compared to the period of 1994–2011) and changes in annual cycle represented by small winter runoff increase and significant summer months decrease (Lamačová et al. 2014). It was in agreement with their previous results from two headwater catchments in the eastern part of the Czech Republic where a decrease by 10–30% was projected for the period of 2071–2100 with a significant decrease in summer months (Benčoková et al. 2011).

The aim of this paper was to analyse the changes in hydrological patterns and shifts in temperature and precipitation that might happen as a result of the projected climate change. Major objectives of the study were: (i) calibration of hydrological model Brook90 (Federer et al. 2003) to the site specific condition of the Bohemian Forest headwater catchment for the control period of 1981–2010, (ii) to simulate the effects of different climate change scenarios on future hydrological pattern in periods of 2021–2050 and 2071–2100, using the calibrated Brook90 model.

Materials and Methods

Catchment characteristics

The catchment (92.7 km^2) is situated on the northern slopes of the Bohemian Forest (Šumava in Czech) mountain range (49°02' N, 13°30' E) and entirely located in the Šumava National Park. The local climate is characterized by high precipitation with high percentage of snow (approximately 40%, according to Langhammer et al. 2015) with mean annual precipitation in the upper parts of the catchment up to 1800 mm yr^{-1} (Starostová 2012). Mean annual temperature at the Churáňov climate station located nearby (1118 m a.s.l., Fig. 1) was 4.8±0.7°C for the period of 1981–2010. Mean elevation of the catchment is 1134 m a.s.l. ranging from 973–1453 m a.s.l., mean slope is 5.8°. The investigated area is a headwater catchment of the Vydra stream and the outlet with water-level recorder operated by the Czech Hydrometeorological Institute (CHMI) is situated in the Modrava municipality downstream the junction of two major catchment streams, Modravský Potok and Roklanský Potok. We thus named the catchment according to the outlet profile as the Modrava catchment, to indicate this part of the Vydra stream that represented the investigated area. Mean annual runoff was 1151 mm (1981–2010).

The bedrock consists of magmatic rocks (granite 29%) and metamorphic rocks mostly gneiss (54%), overlain by quaternary sediments (17%). Soils are dominated by entic and

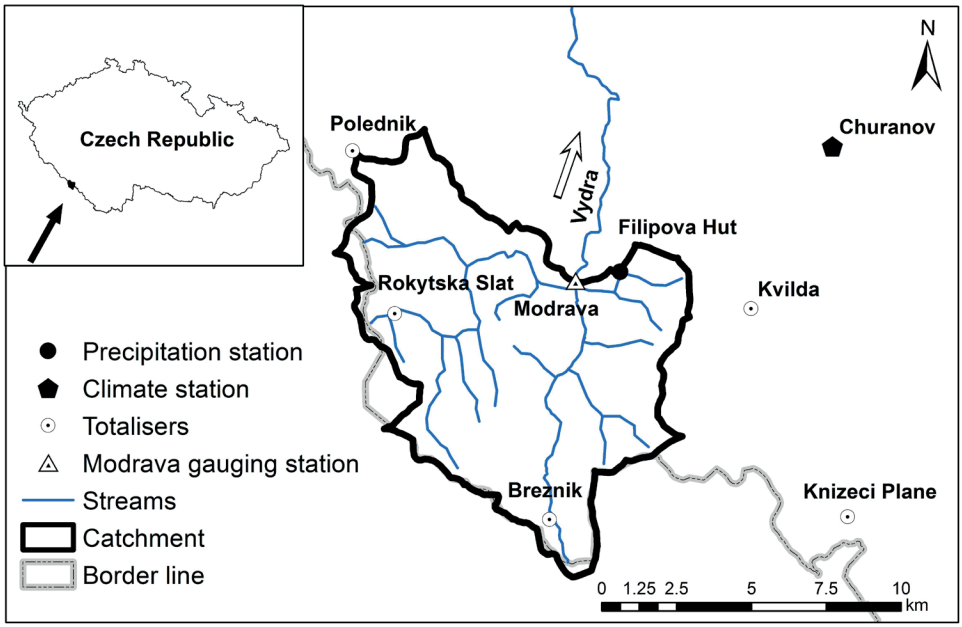

Fig. 1. A map of the study site showing the Modrava catchment and all used precipitation, climate and gauging stations.

typical podzols (47%), permanently or periodically wet soils (46%), Cambisols (3.6%), and Leptosols (3.4%) (Bernsteinová et al. 2015). The catchment is dominantly forested by Norway spruce (*Picea abies* (L.) Karst.) with different age and structure (87%). A small part of forest vegetation (about 5%) consists of mountain ash (*Sorbus aucuparia* L.). Peat bogs are covered with pines *Pinus mugo* Turra and *Pinus mugo* nothosubsp. *rotundata* (Link) Janchen & Neumayer. A small part of mountain meadows is located in the north of the catchment (6%).

Both bark beetle *(Ips typographus* L.) outbreaks and windfall affected the vegetation significantly. The first bark beetle outbreak started around the year 1994 in the southern and south-western part of the catchment along the border with the Bavarian Forest National Park in Germany. Some parts of the forest were left without any intervention, while some other areas were salvaged logged. It resulted into large clear cuts. The second outbreak started after the windstorm Kyrill in the central and eastern part in 2007. It resulted in the mosaic of logged and naturally developed spruce stands. At present, clear cuts occupied 23%, naturally developed stands with dead adult spruces 35%, and living mature stands 33% of the catchment. Wetlands (mostly peat bogs) cover 8% of the catchment (Bernsteinová et al. 2015).

The hydrological modelling

The Brook90 model is a deterministic, process-oriented, lumped parameter hydrological model that was designed to be applicable to any land surfaces at a daily time step year-round (Federer et al. 2003). Brook90 is a parameter-rich model designed primarily to study evapotranspiration and soil water movement at a point, with some provision for stream flow generation by different flow paths. Snow accumulation and melt are controlled by a degree--day method with cold content (Linsley 1949). The model uses the Shuttleworth & Walla-

ce (1985) method for separating transpiration and soil evaporation from sparse canopies, and evaporation of interception. Actual transpiration is reduced below potential when water supply to the plant is limited.

Required inputs to the model are daily precipitation, and maximum and minimum air temperatures. Additional desirable inputs are daily solar radiation and daily mean wind speed, average vapour pressure for the day, and measured runoff (used for calculation of evaluation statistics within the program). Five parameter sets are required: canopy, location; soil (for up to 25 layers); initial and fixed parameters. In this study we did not estimate the course of future vegetation cover changes, and thus we did not modify the future canopy parameters.

The model performance was evaluated by Pearson's correlation coefficient between measured and simulated daily stream flows and by the daily and monthly Nash–Sutcliffe criterion (Nash & Sutcliffe 1970). The model was calibrated on the period of 1981–1999 and validated on the period of 2000–2010.

Meteorological and hydrological data

Meteorological data for the studied catchment (maximum and minimum daily air temperature, daily precipitation, daily mean wind speed and global radiation) were interpolated (using inverse distance weighting as an interpolation method) on the area of the catchment. For the interpolation were used the so called technical series of daily values at a particular grid point (station location) that were calculated from up to 6 neighbouring CHMI stations within a distance of 300 km, with an allowed maximum difference in altitude of 500 m. Before applying inverse distance weighting, data at the neighbour stations were standardized relatively to the altitude of the base grid point (station location). The standardization was carried out by means of linear regression and dependence of values of a particular meteorological element on altitude for each day, individually and regionally Štěpánek et al. (2011). Further details on the data processing can be found also in Štěpánek et al. (2013). The technical series were used also for validation and correction of RCM outputs (Štěpánek et al. 2016). However the mean annual precipitation amount from the technical series was too low (only 1117 mm) compared to measured data (Fig. 2). It would represent rainfall-runoff ratio of 1.05 only, therefore correction had to be used to better represent the catchment precipitation. The station network is sparse in the mountain ridge area and thus we used mean annual data from CHMI rain gauges – totalisers, located at catchment and neighbouring areas

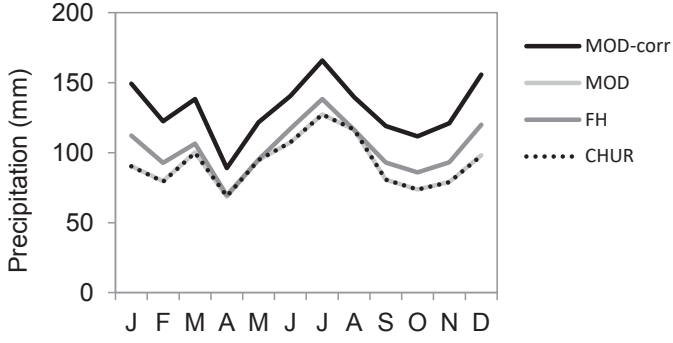

Fig. 2. Annual series of mean precipitation in the period of 1981–2010, MOD-corr – final corrected precipitation, MOD – uncorrected precipitation from "technical" data series (see section Input meteorological and hydrological data for details), FH – Filipova Hut' – CHMI operated precipitation station, CHUR – CHMI operated climate station Churáňov.

(Březník, Rokytská Slať, Knížecí Pláně, Poledník, Kvilda, Filipova Huť; 1981–2010 data and details about the stations are available in Starostová, 2012). The mean annual precipitation from totalisers varied between 1165 mm (Kvilda) and 1845 mm (Březník) with an average of 1487±297 mm. We interpolated the mean annual precipitation amounts (1981–2010) from totalisers from the close vicinity of the Modrava catchment and obtained the mean annual precipitation amount of 1575 mm. The 40% difference corresponds to reports from Slovakia (Lapin et al. 1991) and Switzerland (Sevruk 1985), with the former study showing increase of precipitation totals from April to September by 35–70% when totalisers were used. Based on the comparison of annual precipitation distribution of both Modrava "technical" precipitation series and precipitation data from the CHMI Filipova Huť station (1112 m a.s.l, 49°02' N, 13°31' E) (Fig. 1), we calculated monthly correction factors and increased the precipitation to fit 1575 mm annual mean. The same monthly correction factors were used for future precipitation data.

Runoff data from the CHMI water level gauging station in Modrava (49°02' N, 13°29' E) were used without any corrections.

Future climate projections

Results from simulations performed within the European part of the global Coordinated Regional Climate Downscaling Experiment project (Euro-CORDEX, www.euro-cordex.org) with the 0.11° spatial resolution were used in this study. Experiments were forced by 3 Representative Concentration Pathway (Moss et al. 2010). These scenarios take radiative forcing (W m^{-2}) as the characteristic driving variable, instead of the concentration of the equivalent CO_2 (ppm). RCP represent a wide range of possible future emission scenarios. RCP2.6 assumes that global annual greenhouse gas emissions will peak around 2010–2020 (van Vuuren et al. 2007). RCP4.5 expects emissions to peak around 2040 and then decline (Clarke et al. 2007). RCP6 assumes that the emissions will peak around 2080 (not used in this study) and finally RCP8.5 expects emissions to rise throughout the 21st century (Riahi et al. 2007).

Four regional climate models (RCMs) with three driving global climate models (GCMs) and three different representative concentration pathway RCPs 2.6, 4.5 and 8.5 W m^{-2} scenarios were used. It represents nine plausible future scenarios in total, namely: ALADIN53 (RCM) with CNRM-CM5 driving GCM, RCP 4.5 and RCP 8.5; RACMO22E (RCM) with EC-EARTH driving GCM, RCP 4.5 and RCP 8.5; RCA4 (RCM) with EC-EARTH driving GCM, RCP 2.6, RCP 4.5 and RCP 8.5; and CCLM4-8-17 (RCM) with MPI-ESM-LR driving GCM, RCP 4.5 and 8.5. The datasets were post-processed using a correction method called distribution adjusting by percentiles developed by Štěpánek et al. (2016) that is based on the quantile mapping approach of Déqué (2007). This correction method, based on correction of individual percentiles of empirical distribution, was compared with other bias correction approaches, e.g. in Gutiérrez et al. (2018), and proved to behave very well. Compared to other quantile mapping methods it better focuses on a proper transfer function for tails of the distributions (representation of extremes).

RCM outputs were localized into positions of neighbouring CHMI climate stations and values of such series were then interpolated to obtain spatial information for the catchment. Additional monthly correction factors for precipitation were derived by comparison of technical time series and control run of a given RCM, and the appropriate corrections have been then applied for the future precipitation data. In the presented study, we decided to use two thirty-year periods from the available time series 2021–2100 and compare them to the recent period of 1981–2010. The period of 2021–2050 was chosen as a near future and the period of 2071–2100 was used to represent a more distant future.

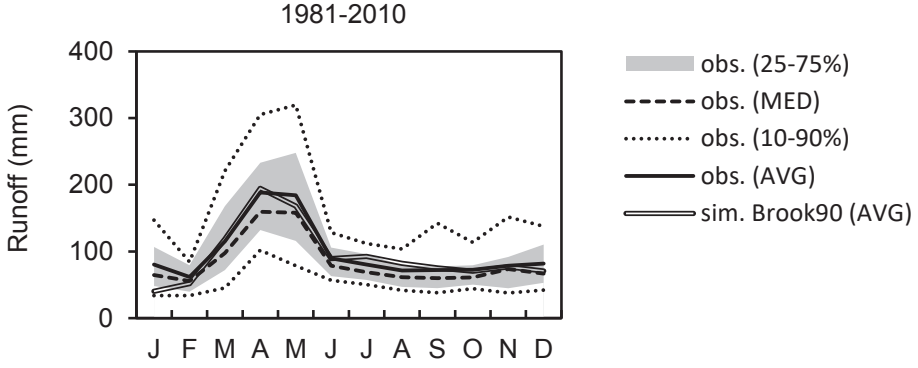

Fig. 3. Mean annual runoff cycle in the control period (1981–2010). Obs. – observed, MED – median, AVG – average, sim. Brook90 – runoff simulated by the Brook90 model, 25–75%: runoff inter-quartile range, 10–90%: runoff inter-quintile range.

Results

Performance of the Brook90 model

The corrected climatic data were used for runoff modelling using the calibrated Brook90 model in the control period 1981–2010. The mean annual runoff from the Modrava catchment calculated from observed data was 1176 mm (±236 mm) and runoff simulated by the Brook90 model was 1158 mm (±236 mm). The Brook90 model also reproduced well mean monthly runoff pattern (Fig. 3). Daily simulated and observed runoffs at the Modrava outlet in the calibration and validation period also were in relatively good agreement (Fig. 4). The Pearson's correlation coefficients were 0.72 (r_{crit} = 0.06, N = 6939, p = 0.05) for daily values and 0.80 (r_{crit} = 0.14, N = 228, p = 0.05) for monthly values in the calibration period (1981–1999). The Pearson's correlation coefficients in the validation period (2000–2010) were 0.80

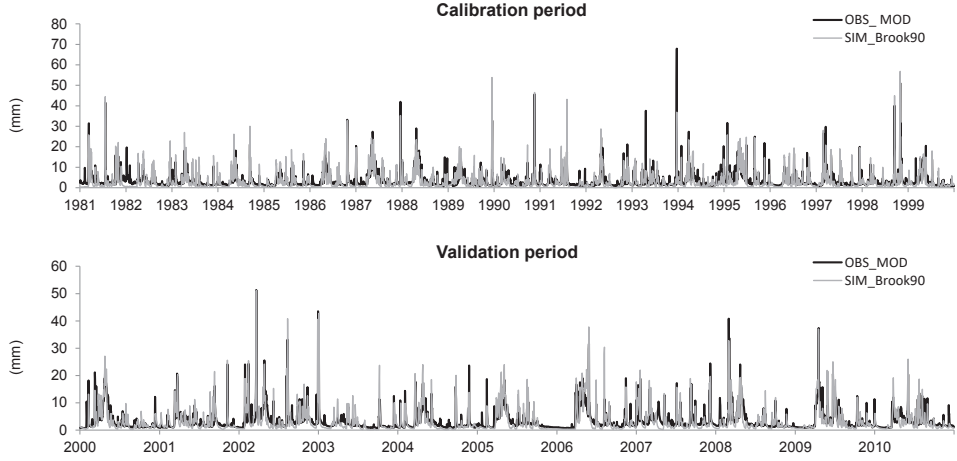

Fig. 4. Comparison of daily observed (OBS_MOD) and simulated (SIM_Brook90) runoff at Modrava outlet in the calibrated and validated period.

(r_{crit} = 0.06, N = 4018, p = 0.05) for daily values and 0.89 (r_{crit} = 0.17, N = 132, p = 0.05) for monthly values.

The Nash-Sutcliffe criterion were 0.43 for daily values and 0.58 for monthly values in the calibration period (1981–1999) and 0.59 for daily values and 0.76 for monthly values in the validation period (2000–2010).

Future temperature projections

Mean annual temperature 4.2°C was measured in the control period (1981–2010). The individual RCM models estimated an increase in mean annual temperature of 0.8–1.8°C for the period of 2021–2050 (compared to the control period of 1981–2010). The RCP 4.5 scenarios projected mean increase of 1.1°C and RCP 8.5 1.4°C (2021–2050) compared to the control period.

All scenarios (with the exception of ALADIN53, RCP 4.5) indicated an increase in November above freezing point in the period of 2071–2100. It increased from −0.3°C during control period (1981–2010) to the interval of 0.5–1.5°C (2071–2100). The summer temperatures are projected to increase notably in July by 0.8–3.1°C to 14.0–16.3°C (2071–2100) (Fig. 5). The projected increase of 1.4–4.9°C in the period of 2071–2100 would result in change of a mean annual temperature from 4.2°C (1981–2010) to 5.4–8.6°C. The RCP 4.5 scenarios projected mean increase of 2.3°C and RCP 8.5 4.2°C compared to the control period. Four of nine scenarios projected an increase of mean monthly temperatures above freezing point in all months and all scenarios expect an increase above freezing point in November and spring March. A notable increase of 1.4–6.5°C is projected for July. It represents an increase from recent 13.2°C (1981–2010) to 14.6–19.7°C (2071–2100) (Fig. 5).

Mean maximum temperatures also showed similar pattern (Fig. 5). RCM models estimated an increase of 0.7–1.7°C from 9.2°C (1981–2010) to 9.9–10.9°C (2021–2050). January mean maximum temperatures are expected to increase by 0.6–2.3°C, while maximum temperatures in July are projected to increase by 0.5–1.0°C only (Fig. 5) in the period of 2021–2050. In the period of 2071–2100, mean maximum temperatures are projected notably higher than in the control period of 1981–2010. The expected increases by 1.0–5.0°C represent temperatures from 10.2–14.2°C. January mean maximum temperatures are projected to be higher by 1.8–6.7°C. July mean maximum temperatures are projected to the increase by 1.3–4.7°C compared to the control period of 1981–2010.

Only minor differences are projected for mean monthly minimum temperatures for the period of 2021–2050 (Fig. 5). Changes of –0.3–0.6°C, compared to mean annual minimum temperature 1.5°C (1981–2010) are projected by RCM models. For the period of 2071–2100 an increase of 0.1–2.4°C in mean annual minimum temperature was projected. An increase in January is projected of 0.3–3.7°C.

Future precipitation projections

The mean annual precipitation amount for Modrava catchment was 1575 mm in the control period of 1981–2010 (Table 1). In general all models projected an increase in annual precipitation amounts. The RCP 2.6 and 4.5 scenarios estimated an increase of 4–17% and RCP 8.5 even of 7–21% for the period of 2021–2050 compared to the control period (1981–2010). Precipitation amounts are expected to increase in almost all months with the exception of March (Fig. 6). Most of the models project decrease by 15% (RCP 2.6 and 4.5) and by 18% (RCP 8.5) on average in March. Scenarios RCP 2.6 and 4.5 expect the largest increase of precipitation from November to January (23%). Scenarios RCP 8.5 expect notable increases from April to June (by 25%) and from October to January (by 25%) (Fig. 6).

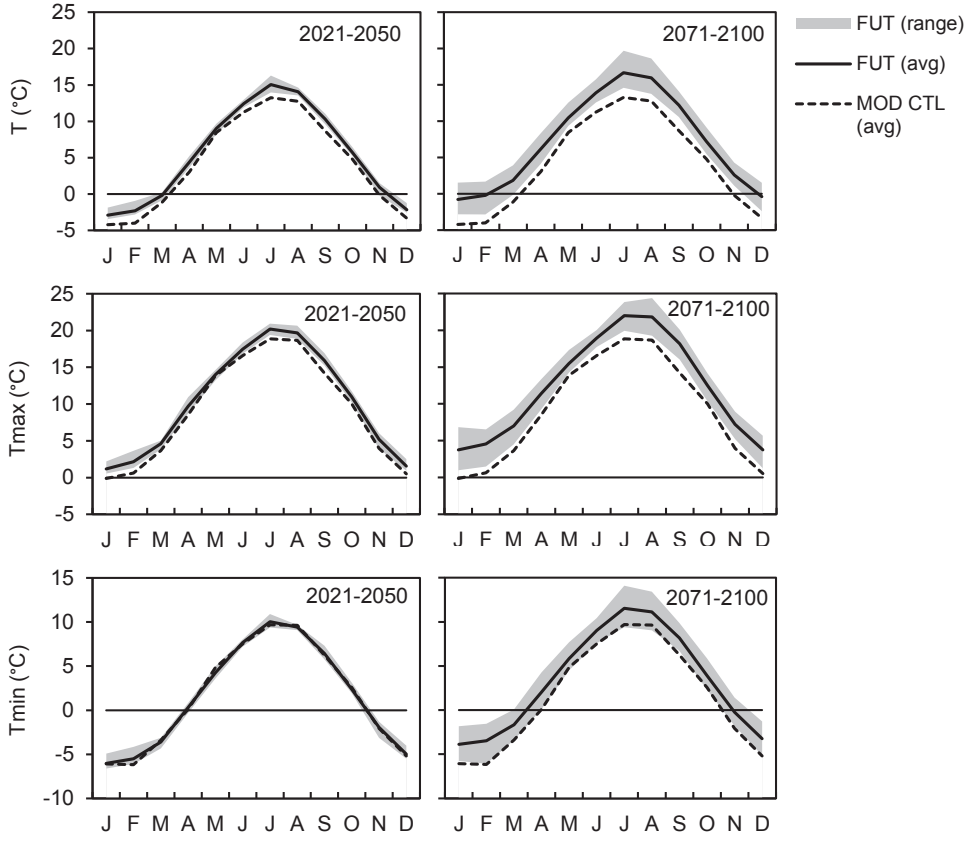

Fig. 5. Annual cycle of monthly mean, maximum and minimum air temperature. FUT – future scenarios (2021–2050 and 2071–2100), MOD ctl – control period (1981–2010). Range based on difference between maximum and minimum RCM simulations for mean temperature, minimum and maximum air temperature.

Also for the period of 2071–2100, the models projected an increase of annual precipitation amounts of 6–22% (RCP 2.6 and 4.5 scenarios) and of 13–27% (RCP 8.5 scenarios) compared to the control period (Table 1). A similar pattern of precipitation changes in the annual distribution as in the period of 2021–2050 was projected for the period 2071–2100. Precipitation amounts are mostly expected to increase with an exception of March and August. March precipitation amounts are projected to decrease by 14% (RCP 2.6 and 4.5 scenarios) and by 6% (RCP 8.5 scenarios). A decrease by 11% is projected for August (RCP 8.5 scenarios). The highest change is projected for winter months – an increase of 26% (RCP 2.6 and 4.5 scenarios) and 36% (RCP 8.5 scenarios) from November to January. A notable increase of 19% (RCP 2.6 and 4.5 scenarios) and 32% (RCP 8.5 scenarios) is also projected from April to June (Fig. 6).

Mean monthly precipitation amounts for the periods of 2021–2050 and 2071–2100 are available in Appendix 1 and 2.

Table 1. Water balance parameters at the investigated catchment for the control period (1981–2010) and two future periods (2021–2050 and 2071–2100). Means ± SD for: P – precipitation, E – evapotranspiration, and Q – runoff; P and Q was measured for control period; all E and future Q were calculated by the Brook90 model.

RCM (driving GCM)	RCP	Period	P (mm y^{-1})	E (mm y^{-1})	Q (mm y^{-1})
Modrava		1981–2010	1575±210	411±29	1176±236
ALADIN53 (CNRM-CM5)	4.5	2021–2050	1840±220	475±26	1357±215
ALADIN53 (CNRM-CM5)	8.5	2021–2050	1910±308	479±33	1431±275
RACMO22E (EC-EARTH)	4.5	2021–2050	1636±248	433±20	1197±233
RACMO22E (EC-EARTH)	8.5	2021–2050	1688±235	438±19	1249±255
RCA4 (EC-EARTH)	2.6	2021–2050	1758±264	466±25	1290±279
RCA4 (EC-EARTH)	4.5	2021–2050	1738±237	477±47	1260±221
RCA4 (EC-EARTH)	8.5	2021–2050	1828±304	479±42	1348±282
CCLM4-8-17 (MPI-ESM-LR)	4.5	2021–2050	1808±354	484±39	1322±305
CCLM4-8-17 (MPI-ESM-LR)	8.5	2021–2050	1802±275	485±28	1315±224
ALADIN53 (CNRM-CM5)	4.5	2071–2100	1919±273	504±28	1417±286
ALADIN53 (CNRM-CM5)	8.5	2071–2100	1996±286	532±30	1466±264
RACMO22E (EC-EARTH)	4.5	2071–2100	1669±233	448±23	1223±227
RACMO22E (EC-EARTH)	8.5	2071–2100	1772±241	477±25	1297±215
RCA4 (EC-EARTH)	2.6	2071–2100	1726±303	461±33	1264±261
RCA4 (EC-EARTH)	4.5	2071–2100	1852±344	568±55	1284±326
RCA4 (EC-EARTH)	8.5	2071–2100	1833±367	532±37	1302±340
CCLM4-8-17 (MPI-ESM-LR)	4.5	2071–2100	1812±328	493±38	1321±264
CCLM4-8-17 (MPI-ESM-LR)	8.5	2071–2100	1913±352	522±33	1392±311

Future evapotranspiration projections

The increase in annual evapotranspiration based on model projections was estimated to be 6 to 19% in the period of 2021–2051. It represents a change from 407 mm (1981–2010) to 433–485 mm (Table 1). Changes in seasonal distribution showed a slight increase for most of the months with absolute maximum in summer months (Fig. 7). RCMs projected an increase of mean annual evapotranspiration from 10 to 40% to 448–569 mm in the period of 2071–2100 (Table 1). The pattern of change showed increase in all of the months with absolute maximum in summer similarly to previous period, with no signs of evapotranspiration reduction due to water availability limitations (Fig. 7).

Mean monthly evapotranspiration for the periods of 2021–2050 and 2071–2100 are available in Appendix 3 and 4.

Future runoff projections

The mean annual runoff for Modrava catchment was 1176 mm in the control period of 1981–2010. The projected precipitation increase resulted in annual runoff increase in all scenarios (Table 1). The RCP 2.6 and 4.5 scenarios estimated an increase of 2–15% and RCP

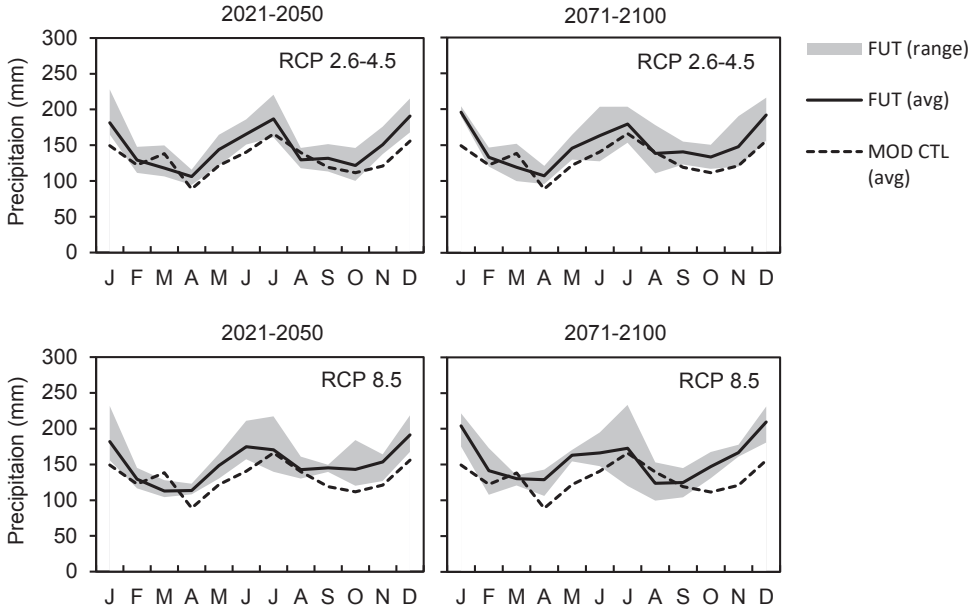

Fig. 6. Mean annual cycle of precipitation. FUT – future scenarios (2021–2050 and 2071–2100), MOD ctl – control period (1981–2010). Range based on difference between maximum and minimum RCM simulations for precipitation.

8.5 scenarios of 6–22% for the period of 2021–2050 compared to the control period (1981–2010). The future and recent monthly medians follow more or less the same pattern in case of RCP 2.6 and 4.5 scenarios however RCP 8.5 scenarios medians show a notable increase of runoff (43%) from October to December in the period of 2021–2050 (Fig. 8).

The RCP 2.6 and 4.5 scenarios projected an increase of 4–20% and RCP 8.5 scenarios of 10–25% in mean annual runoff for the period of 2071–2100 compared to the control period (1981–2010). While the flow pattern in previous period (2021–2050) was similar to control period (1981–2010), the flow pattern in the period of 2071–2100 show a significant shift in annual runoff distribution. A decrease in spring runoff (April to May) by 26% (RCP 2.6 and 4.5) and 34% (RCP 8.5) was projected. The Brook90 simulations using RCMs data showed

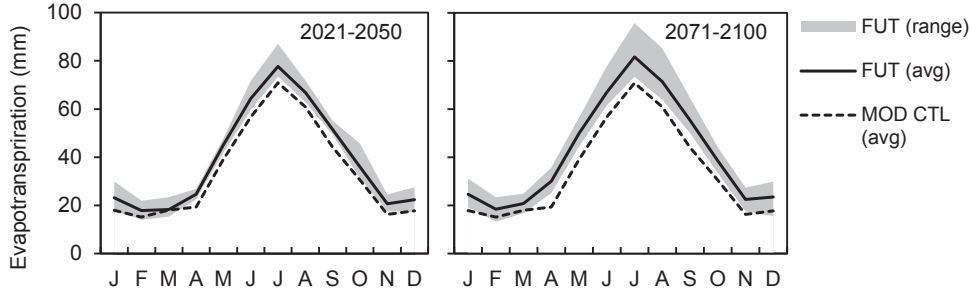

Fig. 7. Mean annual cycle of evapotranspiration. FUT – future scenarios (2021–2050 and 2071–2100), MOD CTL – control period (1981–2010). Range based on difference between maximum and minimum RCM simulations for evapotranspiration.

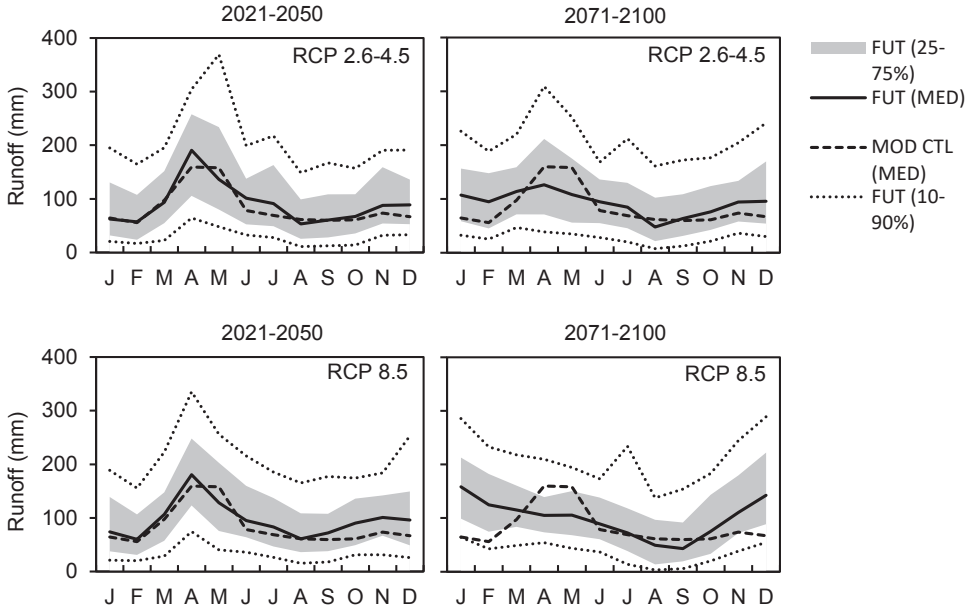

Fig. 8. Mean annual runoff cycle in the future periods (2021–2050 and 2071–2100). FUT – future, 25–75%: runoff inter-quartile range, MOD CTL (MED) – observed median from control period of 1981–2010, FUT 10–90%: future runoff inter-quintile range.

a notable decrease also in August runoff of 22% (RCP 2.6 and 4.5) and 19% (RCP 8.5) and a decrease of 28% in September (RCP 8.5). On the other hand, the winter runoff (January to February) is projected to increase a lot by 60% (RCP 2.6 and 4.5) and even 127% (RCP 8.5) (Fig. 8).

Mean monthly runoff for the periods of 2021–2050 and 2071–2100 are available in Appendix 5 and 6.

Discussion

Estimation of future runoff with a hydrological model using a climate change scenarios is associated with different sources of uncertainties. We assume that in our study one of the major uncertainty is the estimated precipitation input. Precipitation represents the most important variable in hydrological modelling since it affects the runoff generation process directly. Unfortunately, the representative daily record from the catchment was not available and thus the provided data had to be adapted in order to get values that would better represent the precipitation within the catchment. Original values of "technical series" for the precipitation data interpolated from the CHMI station data for the control period of 1981–2010 were too low (mean annual runoff from the Modrava outlet exceed the precipitation amounts in some years). This may be due to the inappropriate location of surrounding rainfall stations that are not much suitable for this particular catchment area and also significant undercatch of the true rainfall reported by numerous previous studies (e.g. Sevruk 1985, Lapin et al. 1991), especially when compared to the totalisers. Our interpolated annual precipitation for the period of 1981–2010 (1575 mm) was slightly higher than the mean annual precipitation value from Langhammer et al. (2015) who estimated mean annual value of 1378

mm for the period of 1961–2010. The difference could be also caused by the selection of different precipitation stations used for their correction. Langhammer et al. (2015) used the CHMI operated precipitation stations providing daily measurements that were not located on the mountain ridge, while we used the totalisers located in higher elevations that should provide more representative values (regarding the long-term means); however, these totalisers provided only annual data. Totaliser data after correction for evaporation were in good agreement with automated station data according to Starostová (2012). The use of totaliser data helped to reduce the bias in total amounts, however, could not be used for the seasonal distribution correction. Although we used mean monthly correction factor based on the difference in seasonal distribution between Churáňov and Filipova Huť stations (Fig. 2), this step of data processing remained highly uncertain. However, such correction was partially verified by a successful runoff simulation for the control period 1981–2010. It is also worth noting that since the Brook90 model is a lumped model, we assumed that the prevailing vegetation cover was Norway spruce and we did not change the vegetation parameters in time, although there were partial changes in vegetation cover during the control period. Bernsteinová et al. (2015) reported that the tree die-off caused by bark beetle outbreak and windfall affected 55% of the catchment by the 2011 year. This approach was chosen based on the results from studies Bernsteinová et al. (2015) and Langhammer et al. (2015) who detected only minor changes in annual runoff and the shifts in spring runoff were attributed rather to temperature increase than vegetation cover change. According to Bernsteinová et al. (2015), the vegetation cover disturbances may not have been rapid enough to generate significant trends in runoff. Regeneration of the surviving vegetation including growing forest stands and secondary structure (shrubs and herbs) can compensate the evapotranspiration losses due to partial tree die-off (Brown et al. 2014).

In respect of climatic modelling, Štěpánek et al. (2016) noted the need of RCM output correction, since the uncorrected RCM data do not capture the Czech climatic conditions well and thus are not directly useful for impact studies. RCM simulations provide outputs that can differ notably (depending e.g. on the driving GCM) and thus use of small number of scenarios for impact studies could be misleading (e.g. Hanel et al. 2012). We assume that use of nine scenarios in this study should represent a sufficiently wide range of future possible climatic conditions.

The mean annual temperature increase for Modrava is similar to the projections for the whole Czech Republic (CR) published by Štěpánek et al. (2016), who used the same RCMs and emission scenarios (plus two additional scenarios compared to our study). Štěpánek et al. (2016) reported the 1°C increase in the period of 2021–2040 and 2.0°C (RCP4.5) and 4.1°C (RCP8.5) for the end of the 21st century. Scenario projections of future precipitation in the Modrava catchment exhibit slightly higher increase compared to the area of CR, where Štěpánek et al. (2016) reported precipitation increase of 7% for the period of 2021–2040, while in our study the projected precipitation increased by 11% (RCP4.5) and 15% (RCP8.5) in the period of 2021–2050. The results by the end of the century were almost the same as for the whole area of CR – an increase of 12% compared to an increase of 13% by Štěpánek et al. (2016) for RCP4.5 and 16% compared to 6–16% for CR (RCP8.5).

A significant winter precipitation increase especially in case of RCP8.5 emission scenarios is similar to the projections for CR by Štěpánek et al. (2016). It represents a change compared to the previous ALADIN-Climate/CZ (using SRES A1B emission scenario) simulations where only a minor winter precipitation increase was projected (Štěpánek et al. 2016). Also the study of Hanel et al. (2012) that evaluated 15 different RCM experiments (using SRES A1B emission scenario) pointed out an uncertainty in winter precipitation increase and did not report any notable changes in mean annual precipitation amounts. The

main change that should occur in the winter precipitation will be in the changes from snow to rain. It will be caused by the temperature increase and occurrence of warmer episodes with a temperature above freezing point. It will lead to notable spring runoff maxima decline up to shifts of runoff maxima to winter in some scenarios. Unavoidably higher winter and spring temperature imply earlier start of growing season that has been already shown across the Czech territory (e.g. Trnka et al. 2015) and in general increase of the transpiration volume in cases when plants are not limited by soil moisture content.

The studies focused on analysis of recent changes in hydrological pattern in the Bohemian Forest area mostly did not found any changes in mean annual runoff (Bernsteinová et al. 2015, Kliment & Matoušková 2009, Langhammer et al. 2015) with the exception of Beudert et al. (2018), who detected an annual runoff decline of 59 mm (for the period from 1978–2013) in the southern slope of the Bohemian Forest. Such a decrease was related to changes in evapotranspiration due to increased temperature.

The projected future mean annual runoff increase does not correspond with the results from previous regional studies that mostly assume runoff decrease as a result of climatic change across different catchment scale from small forested catchments (Benčoková et al. 2011, Lamačová et al. 2014) to mesoscale catchment (Malše River, Němečková et al. 2011). As a reason, we see the use of other RCM models than it used to be in the past. The greatest uncertainty is related to the precipitation projection. There is a big difference between individual RCM and so the difference between RCM and GCM. The projection in such a small area is definitely burdened by a higher uncertainty as it is below the resolution capability of any used RCM, and it is rather necessary to take into account the average projection of the model over a larger area. Generally, despite the bias correction, the climate models can not exactly describe spatial distribution of rainfall changes. This is also one of the reasons why we used in our analysis ensemble of the RCM, which reduces the modelling errors. However, Hanel et al. (2012) estimated a wide range of mean annual runoff changes (prevailingly decrease) across the Czech Republic. It included also estimated increase in northern part of the Czech Republic for the period of 2071–2099. However most of the future runoff changes are similar to our results such as (i) the winter runoff increase caused by shift of runoff maxima from spring snowmelt to winter and (ii) the winter precipitation increase.

Conclusions

We described the impact of nine plausible scenarios of climate change, representing a wide range of possible changes in future anthropogenic greenhouse gas emissions, on forested catchment in the Bohemian Forest in two future periods of 2021–2050 and 2071–2100. The estimated temperature and precipitation increase (especially in winter months) will significantly affect evapotranspiration and runoff. Evapotranspiration is expected to increase as a result of higher temperature and prolongation of the growing season. Mean annual runoff is projected to rise notably as a result of the precipitation increase (despite the increased evapotranspiration rate).

Changes are also modelled for the runoff annual cycle. While in the period of 2021–2050 the annual cycle will not change notably, significant shifts are projected for the period of 2071–2100. A large winter runoff increase and a spring runoff maxima decrease indicate changes in snow cover and snowmelt. Some scenarios even show no spring runoff maxima. Changes are also visible in summer, while the median runoff will not change that much the values of 10 and 25 percentiles (representing of the lowest flows) are notably lower compared to the recent period of 1981–2010.

Acknowledgements. This work was supported by the Interreg Cíl EUS (contract SOSSOD - 164/2017), by the Ministry of Education, Youth and Sports of the Czech Republic – projects LM2015075 and EF16_013/0001782 for the Czech Geological Survey, and National Sustainability Program I (NPU I, project LO1415) for the Global Change Research Institute CAS. MT, PŠ a PZ were supported by the Ministry of Agriculture of the Czech Republic (project QJ1610072: System for monitoring and forecast of impacts of agricultural drought). This research and publication were supported by the Cross-border cooperation programme Czech Republic–Bavaria Free State ETC goal 2014–2020, the Interreg V project No. 26 "Silva Gabreta Monitoring – Implementation of Transboundary Monitoring of Biodiversity and Water Regime".

References

Adams H.D., Guardiola-Claramonte M., Barron-Gafford G.A., Villegas J.C., Breshears D.D., Zou C.B., Troch P.A. & Huxman T.E., 2009: Temperature sensitivity of drought-induced tree mortality portends increased regional die-off under global-change-type drought. *Proceedings of the National Academy of Sciences of the United States of America*, 106: 7063–7066.

Allen C.D., Macalady A.K., Chenchouni H., Bachelet D., McDowell N., Vennetier M., Kitzberger T., Rigling A., Breshears D.D., Hogg E.H. (Ted), Gonzalez P., Fensham R., Zhang Z., Castroj J., Demidova N., Lim J.H., Allard G., Running S.W., Semerci A. & Cobb N., 2010: A global overview of drought and heat-induced tree mortality reveals emerging climate change risks for forests. *Forest Ecology and Management*, 259: 660–684.

Benčoková A., Krám P. & Hruška J., 2011: Future climate and changes in flow patterns in Czech headwater catchments. *Climate Research*, 49: 1–15.

Bernsteinová J., Baessler C., Zimmermann L., Langhammer J. & Beudert B., 2015: Changes in runoff in two neighbouring catchments in the Bohemian Forest related to climate and land cover changes. *Journal of Hydrology and Hydromechanics*, 63: 342–352.

Beudert B., Bernsteinová J., Premier J. & Bässler C., 2018: Natural disturbance by bark beetle offsets climate change effects on streamflow in Bohemian Forest headwater catchments. *Silva Gabreta*, 24: xx–xx.

Brown M.G., Black T.A., Nesic Z., Foord V.N., Spittlehouse D.L., Fredeen A.L., Bowler R., Grant N.J., Burton P.J., Trofymow J.A., Lessard D. & Meyer G., 2014: Evapotranspiration and canopy characteristics of two lodgepole pine stands following mountain pine beetle attack. *Hydrological Processes*, 28: 3326–3340.

Clarke L.,Edmonds J.,Jacoby H., Pitcher H., Reilly J. & Richels R., 2007: *Scenarios of greenhouse gas emissions and atmospheric concentrations. Sub-report 2.1A of Synthesis and Assessment Product 2.1 by the US Climate Change Science Program and the Subcommittee on Global Change Research*. Office of Biological and Environmental Research, US Department of Energy, Washington, DC, 154 pp.

Déqué M., 2007: Frequency of precipitation and temperature extremes over France in an anthropogenic scenario: Model results and statistical correction according to observed values. *Global and Planetary Change*, 57: 16–26.

Federer C.A., Vorosmarty C. & Fekete B., 2003: Sensitivity of annual evaporation to soil and root properties in two models of contrasting complexity. *Journal of Hydrometeorology*, 4: 1276–1290.

Forzieri G., Feyen L., Rojas R., Floerke M., Wimmer F. & Bianchi A., 2014: Ensemble projections of future streamflow droughts in Europe. *Hydrology and Earth System Sciences*, 18: 85–108.

Gutiérrez J.M., Maraun D., Widmann M., Huth R., Hertig E., Benestad R., Roessler O., Wibig J., Wilcke R., Kotlarski S., San Martín D., Herrera S., Bedia J., Casanueva A., Manzanas R., Iturbide M., Vrac M., Dubrovsky M., Ribalaygua J., Pórtoles J., Räty O., Räisänen J., Hingray B., Raynaud D., Casado M.J., Ramos P., Zerenner T., Turco M., Bosshard T., Štěpánek P., Bartholy J., Pongracz R., Keller D.E., Fischer A.M., Cardoso R.M., Soares P.M.M., Czernecki B. & Pagé C., 2018: An intercomparison of a large ensemble of statistical downscaling methods over Europe: Results from the VALUE perfect predictor cross-validation experiment. *International Journal of Climatology*: 1–36. doi.org/10.1002/joc.5462

Hanel M., Vizina A., Máca P. & Pavlásek J., 2012: A multi-model assessment of climate change impact on hydrological regime in the Czech Republic. *Journal of Hydrology and Hydromechanics*, 60: 152–161.

IPCC, 2007: Climate Change 2007. The physical science basis. In: Solomons S., Qin D., Manning M., Chen Z, Marquis M., Averyt K.B., Tignor M. & Miller H.L. (eds): *Contribution of Working Group I to the Fourth Assessment Report of the Intergovernmental Panel on Climate Change*. Cambridge University Press, Cambridge, UK and New York, USA, 996 pp.

IPCC 2013: Climate Change 2013. The physical science basis. In: Stocker T.F., Qin D., Plattner G.K., Tignor M., Allen S.K., Boschung J. Nauels A., Xia Y., Bex V. & Midgley P.M. (eds): *Contribution of Working Group I to the Fifth Assessment Report of the Intergovernmental Panel on Climate Change*. Cambridge University Press, Campridge, UK and New York, USA, 1535 pp.

Kliment Z. & Matoušková M., 2009: Runoff changes in the Šumava Mountains (Black Forest) and the foothill

regions: extent of influence by human impact and climate change. *Water Resources Management*, 23: 1813–1834.

Lamačová A., Hruška J., Krám P., Stuchlík E., Farda A., CHuman T. & Fottová D., 2014: Runoff trends analysis and future projections of hydrological patterns in small forested catchments. *Soil and Water Research*, 9: 169–181.

Langhammer J., Su Y. & Bernsteinová J., 2015: Runoff response to climate warming and forest disturbance in a mid-mountain basin. *Water*, 7: 3320–3342.

Lapin M., Faško P. & Košťálová J., 1991: Zhodnotenie zrážkových pomerov na území Slovenska po korekcii systematických chýb meraní zrážok [Evaluation of atmospheric precipitation on the area of Slovakia after correction of systematic errors in precipitation measurements]. *Vodohospodársky Časopis*, 39: 207–220 (in Slovak).

Linsley R.K., 1949: *Applied Hydrology*. McGraw-Hill, New York, 689 pp.

Moss R.H., Edmonds J.A., Hibbards K.A., Manning M.R., Rose S.K., van Vuuren D.P., Carter T.R., Emori S., Kainuma M., Kram T., Meehl G.A., Mitchell J.F.B., Nakicenovic N., Riahi K., Smith S.J., Stouffer R.J., Thomson A.M., Weyant J.P. & Wilbanks T.J., 2010: The next generation of scenarios for climate change research and assessment. *Nature*, 463: 747–756.

Nahs J.E. & Sutcliffe J.V., 1970: River flow forecasting through conceptual models. 1. A discussion of principles. *Journal of Hydrology*, 10: 282–290.

Němečková S., Slámová R. & Šípek V., 2011: Climate change impact assessment on various components of the hydrological regime of the Malše River basin. *Journal of Hydrology and Hydromechanics*, 59: 131–143.

Raffa K.F., Aukema B.H., Bentz B.J., Carroll A.L., Hicke J.A., Turner M.G. & Romme W.H., 2008: Cross-scale drivers of natural disturbances prone to anthropogenic amplification: The dynamics of bark beetle eruptions. *Bioscience*, 58: 501–517.

Riahi K., Gruebler A. & Nakicenovic N., 2007: Scenarios of long-term socio-economic and environmental development under climate stabilization. *Technological Forecasting and Social Change*, 74: 887–935.

Sevruk B., 1985: Systematischer Niederschlagsmessfehler in der Schweiz. In: *Der Niederschlag in der Schweiz*, Sevruk B. (ed.) Beitrage zur Geologie der Schweiz – Hydrologie Nr. 31, Bern: 65–75.

Shuttleworth W. & Wallace J., 1985: Evaporation from sparse crops – an energy combination theory. *Quarterly Journal of the Royal Meteorological Society*, 111: 839–855.

Starostová, M., 2012: Measuring precipitation using totalisers in Šumava. *Meteorological Bulletin*, 65: 180–183.

Štěpánek P., Zahradníček P. & Farda A., 2013: Experiences with data quality control and homogenization of daily records of various meteorological elements in the Czech Republic in the period 1961–2010. *Idojaras*, 117: 123–141.

Štěpánek P., Zahradníček P., Farda A., Skalák P., Trnka M., Meitner J. & Rajdl K., 2016: Projection of drought-inducing climate conditions in the Czech Republic according to Euro-CORDEX models. *Climate Research*, 70: 179–193.

Štěpánek P., Zahradníček P. & Huth R., 2011: Interpolation techniques used for data quality control and calculation of technical series: an example of a Central European daily time series. *Idojaras*, 115: 87–98.

Trnka M., Brázdil R., Balek J., Semerádová D., Hlavinka P., Možný M., Štěpánek P., Dobrovolný P., Zahradníček P., Dubrovský M., Eitzinger J., Fuchs B., Svoboda M., Hayes M. & Žalud Z., 2015: Drivers of soil drying in the Czech Republic between 1961 and 2012. *International Journal of Climatology*, 35: 2664–2675.

van Vliet M.T.H., Donnelly C., Stromback L., Capell R. & Ludwig F., 2015: European scale climate information services for water use sectors. *Journal of Hydrology*, 528: 503–513.

van Vuuren D.P., den Elzen M.G.J., Lucas P.L., Eickhout B., Strengers B.J., van Ruijven B., Wonink S. & van Houdt R., 2007: Stabilizing greenhouse gas concentrations at low levels: an assessment of reduction strategies and costs. *Climatic Change*, 81: 119–159.

Received: 11 July 2018
Accepted: 28 August 2018

Appendix 1. Annual and monthly precipitation (P, in mm) estimated for investigated catchment (MOD) in the control period of 1981–2010 and future simulated precipitation in the period of 2021–2050 based on different regional climate model data and climate change scenarios.

Model RCM (GCM)	MOD-corrected	ALADIN53 (CNRM-CM5)	ALADIN53 (CNRM-CM5)	RACMO22E (EC-EARTH)	RACMO22E (EC-EARTH)	RCA4 (EC--EARTH)	RCA4 (EC--EARTH)	RCA4 (EC--EARTH)	CCLM4-8-17 (MPI-ESM-LR)	CCLM4-8-17 (MPI-ESM-LR)
P		RCP 4.5	RCP 8.5	RCP 4.5	RCP 8.5	RCP 2.6	RCP 4.5	RCP 8.5	RCP 4.5	RCP 8.5
Period	1981–2010	2021–2050	2021–2050	2021–2050	2021–2050	2021–2050	2021–2050	2021–2050	2021–2050	2021–2050
Jan	149.2	171.7	177.7	165.0	155.8	228.1	172.1	231.7	170.1	162.1
Feb	122.4	136.2	130.4	111.4	145.2	120.6	130.4	116.6	147.8	125.7
Mar	138.4	118.5	108.7	107.3	110.6	107.8	106.4	104.2	149.8	128.0
Apr	89.0	115.8	109.5	96.8	108.1	112.6	94.5	113.8	110.4	123.0
May	121.8	137.6	145.2	121.4	153.2	164.6	156.4	164.5	139.6	130.2
Jun	140.6	186.2	210.9	155.0	157.2	166.4	169.7	165.2	150.9	165.2
Jul	166.0	220.6	217.1	161.1	139.7	173.1	210.8	155.5	168.8	169.4
Aug	139.7	146.2	149.6	143.6	160.8	117.9	121.1	130.2	119.4	130.2
Sep	119.1	133.9	149.4	151.6	143.2	138.1	121.2	139.5	113.3	149.3
Oct	111.6	131.6	144.2	100.2	120.1	117.6	113.6	124.3	146.2	183.9
Nov	121.0	141.4	160.6	137.5	126.7	142.9	156.9	164.0	175.9	162.9
Dec	155.9	200.3	207.1	185.2	167.5	168.0	185.1	218.5	215.3	172.5
Annual	**1575**	**1840**	**1910**	**1636**	**1688**	**1758**	**1738**	**1828**	**1808**	**1802**

Appendix 2. Annual and monthly precipitation (P, in mm) estimated for investigated catchment (MOD) in the control period of 1981–2010 and future simulated precipitation in the period of 2071–2100 based on different regional climate model data and climate change scenarios.

Model RCM (GCM)	MOD-corrected	ALADIN53 (CNRM-CM5)	ALADIN53 (CNRM-CM5)	RACMO22E (EC-EARTH)	RACMO22E (EC-EARTH)	RCA4 (EC--EARTH)	RCA4 (EC--EARTH)	RCA4 (EC--EARTH)	CCLM4-8-17 (MPI-ESM-LR)	CCLM4-8-17 (MPI-ESM-LR)
P		RCP 4.5	RCP 8.5	RCP 4.5	RCP 8.5	RCP 2.6	RCP 4.5	RCP 8.5	RCP 4.5	RCP 8.5
Period	1981–2010	2071–2100	2071–2100	2071–2100	2071–2100	2071–2100	2071–2100	2071–2100	2071–2100	2071–2100
Jan	149.2	195.4	175.2	190.5	198.5	190.0	199.2	221.6	204.2	220.9
Feb	122.4	120.1	159.7	126.5	107.7	141.1	146.6	124.8	131.0	173.0
Mar	138.4	114.4	120.8	106.5	134.9	99.8	122.3	131.1	151.9	134.3
Apr	89.0	121.0	142.9	103.2	106.1	98.2	95.7	128.6	118.2	137.1
May	121.8	148.0	170.4	129.8	169.0	144.0	164.2	154.4	142.9	159.0
Jun	140.6	203.4	194.9	151.2	160.9	154.5	178.9	160.9	127.4	147.7
Jul	166.0	200.8	233.4	177.1	165.5	162.8	203.5	172.0	153.3	120.1
Aug	139.7	177.9	153.1	138.3	130.9	142.4	123.7	112.0	110.6	99.5
Sep	119.1	154.9	127.8	144.5	122.3	140.2	122.9	104.2	139.9	145.0
Oct	111.6	150.4	148.2	125.4	130.9	116.9	145.7	142.2	127.8	167.6
Nov	121.0	143.1	161.1	120.0	164.2	153.0	132.8	163.4	190.4	177.7
Dec	155.9	189.5	208.8	156.1	180.8	183.4	216.2	217.8	214.5	231.3
Annual	**1575**	**1919**	**1996**	**1669**	**1772**	**1726**	**1852**	**1833**	**1812**	**1913**

Appendix 3. Annual and monthly evapotranspiration (E, in mm) calculated by the Brook90 model for the Modrava catchment (MOD) in the control period of 1981–2010 and future simulated evapotranspiration in the period of 2021–2050 calculated by the Brook90 model using different regional climate model data and climate change scenarios.

Model RCM (GCM)	MOD-corrected	ALADIN53 (CNRM-CM5)	ALADIN53 (CNRM-CM5)	RACMO22E (EC-EARTH)	RACMO22E (EC-EARTH)	RCA4 (EC--EARTH)	RCA4 (EC--EARTH)	RCA4 (EC--EARTH)	CCLM4-8-17 (MPI-ESM-LR)	CCLM4-8-17 (MPI-ESM-LR)
E		RCP 4.5	RCP 8.5	RCP 4.5	RCP 8.5	RCP 2.6	RCP 4.5	RCP 8.5	RCP 4.5	RCP 8.5
Period	1981–2010	2021–2050	2021–2050	2021–2050	2021–2050	2021–2050	2021–2050	2021–2050	2021–2050	2021–2050
Jan	17.9	20.6	20.5	19.0	17.8	28.8	25.5	29.9	23.0	22.7
Feb	15.1	15.7	15.9	14.0	16.5	18.0	21.9	18.5	21.4	18.9
Mar	18.0	15.3	15.9	17.3	17.0	17.8	19.3	18.4	23.4	20.4
Apr	19.4	24.7	22.6	24.7	25.5	25.6	22.5	26.8	23.0	26.3
May	39.1	44.1	46.9	43.8	43.9	46.8	44.5	47.8	41.9	45.3
Jun	56.7	71.7	70.2	59.5	60.5	60.3	63.3	62.9	66.6	64.6
Jul	70.9	86.9	87.1	74.1	74.2	75.6	78.4	73.6	75.1	74.3
Aug	60.9	71.9	71.3	62.9	65.0	67.1	65.9	65.3	65.4	66.2
Sep	44.1	49.8	50.8	49.4	49.6	51.0	52.8	50.9	53.7	55.1
Oct	30.6	34.5	35.3	31.3	33.2	33.4	36.6	36.5	37.9	45.7
Nov	16.2	18.6	20.3	17.6	18.0	20.3	21.4	22.8	24.5	22.9
Dec	17.8	21.6	22.1	19.0	17.3	21.5	24.5	25.1	27.5	22.4
Annual	**407**	**476**	**479**	**433**	**438**	**466**	**477**	**479**	**484**	**485**

Appendix 4. Annual and monthly evapotranspiration (E, in mm) calculated by the Brook90 model for the Modrava catchment (MOD) in the control period of 1981–2010 and future simulated evapotranspiration in the period of 2071–2100 calculated by the Brook90 model using different regional climate model data and climate change scenarios.

Model RCM (GCM)	MOD-corrected	ALADIN53 (CNRM-CM5)	ALADIN53 (CNRM-CM5)	RACMO22E (EC-EARTH)	RACMO22E (EC-EARTH)	RCA4 (EC--EARTH)	RCA4 (EC--EARTH)	RCA4 (EC--EARTH)	CCLM4-8-17 (MPI-ESM-LR)	CCLM4-8-17 (MPI-ESM-LR)
E		RCP 4.5	RCP 8.5	RCP 4.5	RCP 8.5	RCP 2.6	RCP 4.5	RCP 8.5	RCP 4.5	RCP 8.5
Period	1981–2010	2071–2100	2071–2100	2071–2100	2071–2100	2071–2100	2071–2100	2071–2100	2071–2100	2071–2100
Jan	17.9	22.5	20.8	20.0	19.3	25.5	28.8	31.2	27.0	26.8
Feb	15.1	15.3	16.6	15.0	13.3	20.1	21.9	20.3	19.8	23.4
Mar	18.0	16.8	18.1	18.0	21.5	17.3	22.6	24.3	24.9	23.9
Apr	19.4	26.7	33.4	27.6	32.4	25.9	31.3	35.7	25.1	32.9
May	39.1	50.1	55.0	46.7	49.4	44.4	56.5	53.1	45.1	49.5
Jun	56.7	75.7	77.8	62.5	63.6	61.5	72.4	62.9	63.2	63.7
Jul	70.9	89.6	95.7	75.5	78.1	74.6	90.2	83.9	73.4	74.4
Aug	60.9	74.4	75.8	65.1	69.4	63.9	85.2	75.7	65.8	67.6
Sep	44.1	55.2	55.4	50.7	52.1	50.0	64.6	53.7	56.3	59.8
Oct	30.6	37.5	39.6	33.5	37.1	33.7	44.2	39.5	38.2	43.3
Nov	16.2	19.4	21.8	17.5	21.2	21.3	21.7	25.3	26.9	27.4
Dec	17.8	21.1	21.8	15.6	19.1	22.6	28.5	26.6	26.9	29.9
Annual	**407**	**504**	**532**	**448**	**477**	**461**	**568**	**532**	**493**	**522**

Appendix 5. Annual and monthly runoff (Q, in mm) measured at the Modrava outlet (MOD) in the control period of 1981–2010 and future simulated runoff from the investigated catchment in the period of 2021–2050 calculated by the Brook90 model using different regional climate model data and climate change scenarios.

Model RCM (GCM)	MOD-corrected	ALADIN53 (CNRM-CM5)	ALADIN53 (CNRM-CM5)	RACMO22E (EC-EARTH)	RACMO22E (EC-EARTH)	RCA4 (EC--EARTH)	RCA4 (EC--EARTH)	RCA4 (EC--EARTH)	CCLM4-8-17 (MPI-ESM-LR)	CCLM4-8-17 (MPI-ESM-LR)
Q		RCP 4.5	RCP 8.5	RCP 4.5	RCP 8.5	RCP 2.6	RCP 4.5	RCP 8.5	RCP 4.5	RCP 8.5
Period	1981–2010	2021–2050	2021–2050	2021–2050	2021–2050	2021–2050	2021–2050	2021–2050	2021–2050	2021–2050
Jan	55.8	89.3	94.5	76.5	75.4	121.3	74.4	152.9	74.9	83.8
Feb	61.8	74.1	85.9	72.3	65.4	90.6	70.7	82.3	67.4	64.8
Mar	115.0	129.8	134.7	97.1	105.8	92.9	92.0	89.7	108.9	135.4
Apr	188.6	167.4	208.5	204.8	200.7	171.9	185.3	163.8	222.9	197.3
May	184.3	183.3	135.9	124.3	164.9	177.7	168.7	145.4	218.5	139.1
Jun	89.7	114.3	142.7	100.4	108.7	116.9	112.7	109.6	88.3	102.6
Jul	80.2	140.6	138.2	84.7	68.6	104.9	136.5	88.8	96.6	95.1
Aug	71.5	79.4	87.9	87.1	90.1	52.5	62.1	71.2	60.7	68.3
Sep	72.0	87.4	87.4	97.9	93.7	86.3	66.7	75.5	56.8	88.3
Oct	72.4	83.8	102.0	70.4	84.9	76.3	66.4	85.9	90.8	126.2
Nov	78.6	90.5	112.0	86.3	89.3	104.1	119.0	124.3	130.6	118.3
Dec	81.8	117.2	101.0	95.5	101.3	95.0	105.8	158.6	105.9	95.9
Annual	**1152**	**1357**	**1431**	**1197**	**1249**	**1290**	**1260**	**1348**	**1322**	**1315**

Appendix 6. Annual and monthly runoff (Q, in mm) measured at the Modrava outlet (MOD) in the control period of 1981–2010 and future simulated runoff from the investigated catchment in the period of 2071–2100 calculated by the Brook90 model using different regional climate model data and climate change scenarios.

Model RCM (GCM)	MOD-corrected	ALADIN53 (CNRM-CM5)	ALADIN53 (CNRM-CM5)	RACMO22E (EC-EARTH)	RACMO22E (EC-EARTH)	RCA4 (EC--EARTH)	RCA4 (EC--EARTH)	RCA4 (EC--EARTH)	CCLM4-8-17 (MPI-ESM-LR)	CCLM4-8-17 (MPI-ESM-LR)
Q		RCP 4.5	RCP 8.5	RCP 4.5	RCP 8.5	RCP 2.6	RCP 4.5	RCP 8.5	RCP 4.5	RCP 8.5
Period	1981–2010	2071–2100	2071–2100	2071–2100	2071–2100	2071–2100	2071–2100	2071–2100	2071–2100	2071–2100
Jan	55.8	109.6	147.9	119.7	149.5	96.9	137.8	184.6	116.1	181.1
Feb	61.8	90.5	151.9	109.1	109.0	105.6	113.4	112.3	95.0	153.4
Mar	115.0	125.4	128.3	114.2	128.3	129.0	132.7	120.7	118.9	131.0
Apr	188.6	172.0	121.2	136.9	115.6	141.9	101.0	99.0	219.6	134.4
May	184.3	131.9	113.4	98.2	117.1	139.1	109.9	106.5	174.0	115.6
Jun	89.7	131.2	122.6	86.8	107.7	99.2	111.3	99.2	75.0	86.8
Jul	80.2	118.4	139.9	102.4	83.2	97.2	126.2	93.5	81.5	59.8
Aug	71.5	101.0	84.4	79.6	74.3	86.1	44.3	47.4	48.1	44.0
Sep	72.0	103.0	75.6	86.4	63.5	80.8	48.0	49.6	72.0	67.5
Oct	72.4	106.1	97.0	91.4	84.7	77.4	86.2	80.7	83.9	107.8
Nov	78.6	107.6	119.8	91.6	122.5	102.3	109.0	128.0	125.1	147.2
Dec	81.8	120.1	164.3	106.6	141.1	108.7	164.0	180.9	112.1	163.5
Annual	**1152**	**1417**	**1466**	**1223**	**1297**	**1264**	**1284**	**1302**	**1321**	**1392**